HHS Public Access

Author manuscript

Cortex. Author manuscript; available in PMC 2018 March 01.

Published in final edited form as:

Cortex. 2017 March ; 88: 19–31. doi:10.1016/j.cortex.2016.11.016.

Transcranial direct-current stimulation modulates offline visual oscillatory activity: A magnetoencephalography study

Elizabeth Heinrichs-Graham[a,b,c], **Timothy J. McDermott**[b], **Mackenzie S. Mills**[b], **Nathan M. Coolidge**[b], and **Tony W. Wilson**[a,b,c,CA]

[a]Department of Neurological Sciences, University of Nebraska Medical Center (UNMC), Omaha, NE, USA

[b]Center for Magnetoencephalography, UNMC, Omaha, NE, USA

[c]Department of Pharmacology and Experimental Neuroscience, UNMC, Omaha, NE, USA

Abstract

Transcranial direct-current stimulation (tDCS) is a noninvasive neuromodulatory method that involves delivering low amplitude, direct current to specific regions of the brain. While a wealth of literature shows changes in behavior and cognition following tDCS administration, the underlying neuronal mechanisms remain largely unknown. Neuroimaging studies have generally used fMRI and shown only limited consensus to date, while the few electrophysiological studies have reported mostly null or counterintuitive findings. The goal of the current investigation was to quantify tDCS-induced alterations in the oscillatory dynamics of visual processing. To this end, we performed either active or sham tDCS using an occipital-frontal electrode configuration, and then recorded magnetoencephalography (MEG) offline during a visual entrainment task. Significant oscillatory responses were imaged in the time-frequency domain using beamforming, and the effects of tDCS on absolute and relative power were assessed. The results indicated significantly increased basal alpha levels in the occipital cortex following anodal tDCS, as well as reduced occipital synchronization at the second harmonic of the stimulus-flicker frequency relative to sham stimulation. In addition, we found reduced power in brain regions near the cathode (e.g., right inferior frontal gyrus) following active tDCS, which was absent in the sham group. Taken together, these results suggest that anodal tDCS of the occipital cortices differentially modulates spontaneous and induced activity, and may interfere with the entrainment of neuronal populations by a visual-flicker stimulus. These findings also demonstrate the importance of electrode configuration on whole-brain dynamics, and highlight the deceptively complicated nature of tDCS in the context of neurophysiology.

[CA]Corresponding Author: Tony W. Wilson, Ph.D., Center for Magnetoencephalography, University of Nebraska Medical Center, 988422 Nebraska Medical Center, Omaha, NE 68198-8422, Phone: (402) 552-6431, Fax: (402) 559-5747, Tony.W.Wilson@gmail.com.

Keywords

cortex; oscillations; entrainment; neuromodulation; alpha

1. Introduction

Transcranial direct-current stimulation (tDCS) is a neuromodulatory method that involves delivering low amplitude, direct-current to specific areas of the brain using sponges or small electrodes. Typically, two electrodes are used and the low amplitude current creates a current-loop through the brain running from one electrode (i.e., the anode) to the other electrode (i.e., the cathode), altering the neural environment within the path of the loop. The stimulation is not believed to induce action potentials, but does modulate the excitability of the underlying neuronal tissue, likely by modifying the local ionic environment around neurons (Coffman, Clark, & Parasuraman, 2014; Fertonani & Miniussi, 2016; Filmer, Dux, & Mattingley, 2014; Liebetanz, Nitsche, Tergau, & Paulus, 2002; Nitsche, Nitsche, et al., 2003; Nitsche & Paulus, 2000, 2001). However, importantly, the exact nature of these effects seems to depend on many factors, including duration and intensity of stimulation, size of electrode sponges, positioning of the anode and cathode (in absolute terms, as well as relative to the other), the state of the cortical area being stimulated, and many other factors (see (Fertonani & Miniussi, 2016)). tDCS is safe in humans, with only rare, minimal side effects that include mild tingling or itching sensations under the electrodes, slight fatigue, mild skin irritation, and headache (Nitsche, Liebetanz, et al., 2003; Poreisz, Boros, Antal, & Paulus, 2007; Woods et al., 2016). These side effects quickly subside after termination of tDCS.

Extensive behavioral studies have examined how tDCS affects visual processing. In healthy participants, this work has shown that anodal tDCS applied to visual cortex enhances visual detection (Kraft et al., 2010; Olma, Kraft, Roehmel, Irlbacher, & Brandt, 2011), reduces phosphene detection thresholds (Antal, Kincses, Nitsche, & Paulus, 2003; Lang et al., 2007), improves the perception of faces (Barbieri, Negrini, Nitsche, & Rivolta, 2016; Renzi et al., 2015) and objects (Barbieri et al., 2016), increases visual working memory performance (Barbieri et al., 2016; Makovski & Lavidor, 2014), and facilitates visuo-motor coordination (Antal, Nitsche, et al., 2004). Further, recent work demonstrates that tDCS of the occipital cortex may also have therapeutic benefits. For example, Ding and colleagues (2016) applied tDCS to the occipital cortex of adults with amblyopia, a developmental visual disorder that may result in the loss of visual acuity, depth perception, and contrast detection in the affected eye, and found that anodal stimulation accentuated visual evoked potentials, increased visual acuity, and improved contrast sensitivity in both controls and patients with amblyopia (Z. Ding et al., 2016). The opposite pattern was shown after cathodal stimulation, whereas no effects were seen after sham stimulation. Furthermore, visual acuity improvements persisted 48 hours after anodal stimulation in patients (Z. Ding et al., 2016). A similar but smaller study from the same group also found improved contrast sensitivity following occipital anodal tDCS in patients with amblyopia, coupled with a reduction in pathological asymmetry in occipital activation during visual stimulation, as measured by fMRI (Spiegel, Byblow, Hess, & Thompson, 2013). Finally, tDCS studies in patients with

hemianopia (i.e., blindness to one visual hemi-field following a brain insult) have shown significantly greater visual field recovery following a combination of occipital anodal tDCS and visual restoration therapy (VRT), compared to the effects of sham stimulation with VRT, or VRT alone (Plow, Obretenova, Fregni, Pascual-Leone, & Merabet, 2012; Plow, Obretenova, Jackson, & Merabet, 2012).

While it is clear that anodal tDCS over the occipital cortices consistently results in vision enhancement, discovery of the neurophysiological underpinnings of such effects has proven difficult. Investigators have attempted to quantify the nature of tDCS effects on physiology using EEG (e.g., (Gall et al., 2015; Reinhart & Woodman, 2015; Reinhart, Zhu, Park, & Woodman, 2015)), fMRI (e.g., (Alekseichuk, Diers, Paulus, & Antal, 2015; Amadi, Ilie, Johansen-Berg, & Stagg, 2013; Antal, Polania, Schmidt-Samoa, Dechent, & Paulus, 2011; Hilgenstock, Weiss, Huonker, & Witte, 2016; Hunter et al., 2015; Spiegel et al., 2013)), and MEG (Garcia-Cossio et al., 2015; Hanley, Singh, & McGonigle, 2015; Marshall, Esterer, Herring, Bergmann, & Jensen, 2015; Soekadar et al., 2013). However, there has been little consensus across studies, especially those with similar task parameters. Basically, there are several imaging studies that show little-to-no stimulation effect and, more importantly, the literature is full of contradictory results with very few replications. Of particular relevance to the current study, research shows that anodal tDCS over the occipital cortices increases offline visual evoked potentials (Antal, Kincses, Nitsche, Bartfai, & Paulus, 2004; Strigaro, Mayer, Chen, Cantello, & Rothwell, 2015), as well as online BOLD activation during visual perception (Alekseichuk et al., 2015). However, two recent MEG-tDCS studies attempted to identify online oscillatory alterations in the visual cortex during occipital tDCS, and both reported largely null results (Hanley et al., 2015; Marshall et al., 2015). In fact, the eloquent study by Hanley and colleagues showed that occipital gamma oscillations were only modulated during tDCS when the stimulation was applied using an electrode configuration distant from the occipital cortex (i.e., involving the motor and frontal cortices, (Hanley et al., 2015)), whereas the study by Marshall et al. reported no differences in induced oscillatory during anodal or cathodal occipital stimulation (Marshall et al., 2015). Only two other studies have utilized tDCS and MEG, but the goal of these studies was to evaluate whether online tDCS artifacts precluded accurate MEG source reconstruction (Garcia-Cossio et al., 2015; Soekadar et al., 2013). Both studies found that tDCS artifacts could be effectively removed from the MEG signals to enable accurate localization of responses (Garcia-Cossio et al., 2015; Soekadar et al., 2013). Further, one of these studies found that tDCS applied to the primary motor cortex altered slow wave activity (0-4 Hz) in several brain regions (Garcia-Cossio et al., 2015). It is important to emphasize that these studies utilized a concurrent MEG-tDCS or “online” design, and the lasting offline effects of tDCS on neuromagnetic activity remain unresolved but are likely present (for a review, see (Stagg & Nitsche, 2011)). For example, a recent study of motor activity showed that the maximal effects of tDCS on motor-evoked potentials occurred at least 15 to 30 minutes after the cessation of stimulation (Kuo et al., 2013). However, it is not clear whether this temporal profile would be similar for sensory-specific areas or association cortices serving cognition.

The primary goal of the current study was to identify offline tDCS-induced alterations in the oscillatory dynamics of visual entrainment. We utilized a visual entrainment task because it enabled the parallel examination of strong neuronal responses in multiple frequency bands

(Heinrichs-Graham & Wilson, 2012). To this end, we performed either active or sham tDCS using an occipital-frontal electrode configuration on healthy participants who were viewing an animated movie, and then recorded MEG during an offline visual entrainment task. We used this occipital-frontal electrode configuration to maximize stimulation of the occipital cortices, while minimizing electrical current shunting through the scalp. We also focused on the offline effects of tDCS, as previous MEG studies have shown that online effects are small or nonexistent (Hanley et al., 2015; Marshall et al., 2015) and some evidence suggests that offline effects may be more robust (for a review, see (Stagg & Nitsche, 2011)). Finally, the animated movie allowed us to control the context and engage occipital neurons throughout tDCS. The resulting MEG data were transformed into the time-frequency domain, and significant oscillatory responses were imaged using beamforming. The effects of tDCS on absolute and relative power in specific brain circuits were then assessed. We hypothesized that there would be oscillatory differences at the stimulation sites, as well as regions that were functionally and anatomically connected to these sites.

2. Methods

2.1 Participant Selection

We studied 35 healthy participants (16 females; 3 left-handed), all of whom were recruited from the local community. The mean age was 24.23, with a range of 20-32 years-old. Exclusionary criteria included any medical illness affecting CNS function (e.g., HIV/AIDS), neurological or psychiatric disorder, history of head trauma, current substance abuse, and the MEG Laboratory's standard exclusion criteria (e.g., any type of ferromagnetic implanted material). After complete description of the study was given to participants, written informed consent was obtained following the guidelines of the University of Nebraska Medical Center's Institutional Review Board, which approved the study protocol.

Once participants were consented, they were randomly assigned to sham (16 participants, 8 female) and active (19 participants, 8 female) stimulation groups. Participants were blinded to their group identification. The two groups were matched on age (sham: 24.0 years; active: 24.4 years), sex, handedness, ethnicity, and educational level. With the exception of stimulation (active or sham), all participants completed the same experimental protocol.

2.2 Transcranial Direct-Current Stimulation (tDCS)

The 5 × 7 cm anode pad was positioned over midline occipital cortex near the calcarine fissure, while the 5 × 7 cm cathode pad was positioned over the right prefrontal cortices, near the area generally referred to as supraorbital in most tDCS studies. Each tDCS sponge was soaked in 12 mL of saline solution and positioned on the head using the International 10/20 system (Jasper, 1958; Klem, Luders, Jasper, & Elger, 1999) (Jasper, 1958), which is commonly employed in EEG, fNIRS, and tDCS studies (e.g., (Wilson, Kurz, & Arpin, 2014)). First, the distance from the nasion to the inion was measured and a mark was made on the scalp at the 50% point, then the distance between the left and right periauricles was measured and the midpoint was marked. The intersection of the inion/nasion plane and the periaruicle plane is, by definition, Cz. In our experiment, the anode was positioned on the midline and centered about 12.5% above the inion, which corresponds to ~2.5% superior to

Oz, while the cathode was centered directly lateral to Fp2 by ~7.5%. This electrode configuration was based on calculations from a series of studies by Okamoto and colleagues (Okamoto et al., 2004; Okamoto & Dan, 2005), who developed a method for transforming the scalp-based International 10-20 coordinate system to Montreal Neurological Institute (MNI) based coordinates. Briefly, using a data from a large sample of healthy adults, they developed a probabilistic distribution of the cortical projection points in MNI space that corresponds to input coordinates from the International 10-20 system (Okamoto et al., 2004). Based on their data, coordinates in the International 10-20 system (i.e., scalp-based) can be estimated in MNI space with an average standard deviation of 8 mm (Okamoto et al., 2004), which is almost negligible given the size of our 5 × 7 cm tDCS sponges. Thus, we computed the coordinates of each of our sponges in the International 10-20 system, and then used the transformation methods provided by Okamoto et al. (Okamoto et al., 2004) to obtain the MNI coordinates that corresponded to these scalp based locations. These data indicated that the anode was near the calcarine fissure, while the cathode was over right prefrontal cortices.

Participants in the active stimulation group underwent 20 minutes of 2.0 mA direct-current stimulation, plus ~30 s ramp-up and ramp-down periods, while passively viewing an animated movie. The sham group received the same passive visual experience for 20 minutes, but no stimulation outside of the ~30 s ramp periods, which were meant to mimic the tingling effects of active stimulation so that participants were not privy to their group identification. A Soterix Medical (New York, New York, USA) tDCS system was used for stimulation. Following active/sham stimulation, participants were prepared for MEG recording and seated with their head positioned within the MEG helmet. The overall setup took about 15 minutes from the stop of stimulation to the initiation of the MEG session. This time interval was by design and likely reasonable for detecting post-stimulation effects, given the findings of Kuo et al. (Kuo et al., 2013). Briefly, this study found that the level of cortical excitability in the motor cortex peaks 15 to 20 minutes after the cessation of tDCS, and then slowly dissipates over the next 70 minutes. Thus, we aligned our MEG recording session to coincide with this period of maximal excitability, although we acknowledge that Kuo et al.'s findings may not directly extend beyond the motor cortex.

2.3 Experimental paradigm and stimuli

During MEG recording, participants were seated in a nonmagnetic chair within the magnetically-shielded room (MSR) with both arms resting on a table attached to the chair body. Ambient lighting in the MSR was equal throughout and slightly dimmed. Participants were instructed to remain still and fixate on a small white circle that flickered at 15 Hz. The white circle was 3.8 cm in diameter and presented centrally on a black background. The 15 Hz flicker train lasted for 1.5 s, and the inter-stimulus interval was 2.5 s to 3.0 s. Each participant completed 120 trials, which resulted in a total recording time of about 9 minutes.

2.4 MEG data acquisition & coregistration with structural MRI

All recordings were conducted in a one-layer magnetically-shielded room with active shielding engaged. Neuromagnetic responses were sampled continuously at 1 kHz with an acquisition bandwidth of 0.1–330 Hz using a 306-sensor Elekta MEG system (Elekta,

Helsinki, Finland). MEG data from each individual were corrected for head motion and subjected to noise reduction using the signal space separation method with a temporal extension (tSSS; (Taulu & Simola, 2006; Taulu, Simola, & Kajola, 2005)). Each participant's MEG data were then coregistered with high-resolution structural T1-weighted MRI data prior to the application of source space analyses (i.e., beamforming) using BESA MRI (Version 2.0). These neuroanatomic images were acquired with a Philips Achieva 3T X-series scanner using an eight-channel head coil and a 3D fast field echo sequence with the following parameters: TR: 8.09 ms; TE: 3.7 ms; field of view: 24 cm; slice thickness: 1 mm with no gap; in-plane resolution: 1.0 × 1.0 mm; sense factor: 1.5. The structural volumes were aligned parallel to the anterior and posterior commissures and transformed into standardized space. Following the beamformer analyses, each subject's functional images were transformed into standardized space by using the transform that was previously applied to the structural MRI volume and spatially resampled.

2.5 MEG preprocessing, time-frequency transformation, & sensor-level statistics

Cardio-artifacts were removed from the data using signal-space projection (SSP), which was accounted for during source reconstruction (Uusitalo & Ilmoniemi, 1997). The continuous magnetic time series was divided into epochs of 3.6 s duration, with the baseline defined as −0.6 to 0.0 s before stimulus onset. Epochs containing artifacts were rejected based on a fixed threshold method, supplemented with visual inspection. Artifact-free epochs were transformed into the time-frequency domain using complex demodulation (resolution: 0.5 Hz, 100 ms from 5 to 80 Hz; (Papp & Ktonas, 1977)), and the resulting spectral power estimations per sensor were averaged over trials to generate time-frequency plots of mean spectral density. These sensor-level data were normalized by dividing the power value of each time-frequency bin by the respective bin's baseline power, which was calculated as the mean power during the −0.6 s to 0.0 s pre-stimulus time period.

The specific time-frequency windows used for imaging were determined by statistical analysis of the sensor-level spectrograms across the entire array of gradiometers and all participants. Each data point in the spectrogram was initially evaluated using a mass univariate approach based on the general linear model (GLM). To reduce the risk of false positive results while maintaining reasonable sensitivity, a two stage procedure was followed to control for Type 1 error. In the first stage, one-sample t-tests were conducted on each data point and the output spectrogram of t-values was thresholded at $p < 0.05$ to define time-frequency bins containing potentially significant oscillatory deviations across all participants. In stage two, time-frequency bins that survived the threshold were clustered with temporally and/or spectrally neighboring bins that were also above the ($p < 0.05$) threshold and a cluster value was derived by summing all of the t-values of all data points in the cluster. Nonparametric permutation testing was then used to derive a distribution of cluster values, and the significance level of the observed clusters (from stage one) were tested directly using this distribution (Ernst, 2004; Maris & Oostenveld, 2007). For each comparison, at least 10,000 permutations were computed to build a distribution of cluster values. Based on these analyses, time-frequency windows that contained a significant oscillatory event across all participants were subjected to the beamforming analysis.

2.6 MEG imaging & statistics

Cortical networks were imaged through an extension of the linearly constrained minimum variance vector beamformer (Gross et al., 2001; Van Veen, van Drongelen, Yuchtman, & Suzuki, 1997), which employs spatial filters in the frequency domain to calculate source power for the entire brain volume. The single images were derived from the cross spectral densities of all combinations of MEG gradiometers averaged over the time-frequency range of interest, and the solution of the forward problem for each location on a grid specified by input voxel space. Following convention, the source power in these images was normalized per participant using a separately averaged pre-stimulus noise period of equal duration and bandwidth (Hillebrand, Singh, Holliday, Furlong, & Barnes, 2005). MEG pre-processing and imaging used the Brain Electrical Source Analysis (BESA version 6.0) software.

Normalized source power was computed for the selected time-frequency bands over the entire brain volume per participant at 4.0 × 4.0 × 4.0 mm resolution. The resulting 3D maps of brain activity were statistically evaluated using a random-effects, mass univariate approach based on the GLM. Task effects were examined separately in each group using one-sample t-tests, whereas the effect of group (i.e., active vs. sham) was determined using two-tailed independent-samples t-tests per time-frequency bin. All output statistical maps were displayed as a function of alpha level, and adjusted for multiple comparisons using a spatial extent threshold (i.e., cluster restriction; $k = 300$ contiguous voxels) based on the theory of Gaussian random fields (Poline, Worsley, Holmes, Frackowiak, & Friston, 1995; 1999; Worsley et al., 1996). Maps of task effects were thresholded at $p < 0.001$, corrected, while group difference maps were thresholded at $p < .01$, corrected.

2.7 Peak voxel extraction and analysis

We extracted virtual sensors corresponding to the peak voxel for significant effects in the occipital region, as these cortices were closest to the anode and showed robust group differences. Briefly, we identified the peak voxel by conducting a one-sample t-test across both groups for each frequency band. This t-test yielded a SPM and we selected the voxel in each hemisphere with the highest t-value per significant cluster for virtual sensor extraction. To create the virtual sensors, we applied the sensor weighting matrix derived through the forward computation to the preprocessed signal vector, which yielded a time series for the specific coordinate in source space. Note that this virtual sensor extraction was done per participant, once the coordinates of interest (i.e., one per cluster) were known. Once these virtual sensors were extracted, absolute and relative activity values were computed and subjected to statistical analyses.

3. Results

All participants completed the task successfully. One sham and two active participants were excluded from all statistical analyses due to excessive artifacts in their MEG data. There were no significant differences between the final groups in regards to sex, $\chi^2(1, N = 32) = 1.05$, $p = .31$, or age, $t(30) = 0.321$, $p = .75$.

3.1 Sensor-level results

Sensor-level time-frequency spectrograms across all participants indicated significant oscillatory responses in a large number of posterior sensors at the flicker frequency (14-16 Hz, 0.1-2.0 s; $p < .0001$, corrected), as well as the second harmonic (29-31 Hz, 0.1-2.0 s; $p < .0001$, corrected), third harmonic (44-46 Hz, 0.2-2.0 s; $p < .0001$, corrected), and the fifth harmonic (74-76 Hz, 0.3-2.0 s; $p < .0001$, corrected), all of which were increases or synchronization (ERS) responses. Of note, we were unable to resolve a significant response at 60 Hz, potentially because this is the mains power frequency in the United States. There were also significant alpha (10-13 Hz) and beta (17-22 Hz) desynchronization (ERD) responses that emerged from 0.2 s to 2.1 s in a large portion of posterior sensors (both p's < .0001, corrected). All of these responses are shown in Figure 1. Time-frequency bins containing the maximum power for each response (fundamental: 14-16 Hz, 0.9-1.5 s; second harmonic: 29-31 Hz, 0.9-1.5 s; third harmonic: 44-46 Hz, 0.9-1.5 s; fifth harmonic: 74-76 Hz, 0.9-1.5 s; alpha ERD: 10-13 Hz, 0.4-0.8 s; beta ERD: 17-22 Hz, 0.4-0.8 s), and a window of equal bandwidth and duration from the baseline period, were independently imaged per participant using beamforming to determine the precise brain regions generating each significant oscillatory response. All further analyses, including tDCS effects, were examined in source space.

3.2 Beamforming results

3.2.1 Visual flicker responses at the fundamental and harmonic frequencies—

As described in the methods, one-sample t-tests were performed on each group and time-frequency bin to investigate task effects, while two-sample t-tests were used to probe group effects. Analysis of task effects showed significant ERS responses in the bilateral medial occipital cortices at the fundamental, second harmonic, third harmonic, and fifth harmonic frequencies in both groups (all p's < .001, corrected; Figure 2). These neuronal responses involved highly overlapping areas of occipital cortices across both groups and all four frequency bins. Interestingly, only the second harmonic (30 Hz) showed between-group differences, with the active group having a significantly reduced response compared to the sham group ($p < .01$, corrected; Figure 3). In addition, both groups exhibited significant ERS in the cerebellum bilaterally ($p < .001$, corrected) for each harmonic, yet not the fundamental (15 Hz) response. However, like the medial occipital ERS, group differences were only observed for the second harmonic (30 Hz) and these reflected stronger ERS responses in the left cerebellum of the sham relative to the active stimulation group ($p < .01$, corrected).

There were also many significant responses distant from the anodal stimulation region, which are all described in Table 1. For example, at the fundamental flicker frequency, there was a significant ERD in the right inferior frontal gyrus (IFG) of the active group that was absent in the sham group, which resulted in a significant group effect in this area ($p < .01$, corrected; Figure 4). At the second harmonic, the sham group had significant ERS responses in the left superior frontal gyrus, left prefrontal cortex (PFC), medial PFC, supplementary motor area bilaterally, right superior parietal cortex, and other brain regions (see Table 1; $p < .001$, corrected). The active group had a similar pattern of responses, although activity was weaker in several brain regions and this resulted in significant between-group differences in

the regions described above (i.e., occipital and cerebellum), as well as the right parietal cortices, left medial PFC, and the left SMA (all *p*'s < .01, corrected).

At the third harmonic, both groups showed ERS responses in the posterior cingulate and right posterior parietal cortex (both *p*'s < .001, corrected), with the sham group having significantly stronger ERS activity relative to the active group in the parietal cortex ($p < .01$, corrected). As with the fundamental, the active group exhibited a significant ERD in the right IFG ($p < .001$, corrected) at the third harmonic frequency (45 Hz), which resulted in a significant between-groups effect in this region ($p < .01$, corrected; Figure 4). At the fifth harmonic, the active group again showed significant ERD activity in the right IFG ($p < .001$, corrected), which was absent in the sham group resulting in another group effect in this region ($p < .01$, corrected; Figure 4). There were also significant between-group differences in the right precentral gyrus ($p < .01$, corrected), where the sham group showed an additional ERS peak ($p < .001$, corrected) that was absent in the active group.

3.2.2 Visual flicker side-band response—As mentioned above, there were significant responses in the side bands above and below the fundamental response, which were essentially alpha (below) and beta (above) ERD responses. Imaging these two bands revealed significant activity throughout the occipital, parietal, and cerebellar cortices bilaterally, with peak responses found in the lateral occipital and cerebellar cortices ($p < .001$, corrected). None of these alpha and beta responses differed between groups. Interestingly, the alpha and beta ERD appeared to "wrap around" the fundamental and harmonic ERS responses (see Figure 2). Finally, in the beta frequency range, there were significant group effects in the left medial PFC and other regions, which resulted from the active group exhibiting significant ERD in these regions that were absent in the sham group. Additional regions that were significantly active in one or both groups are shown in Table 1, where significant task and group effects are listed.

3.2.3 Effects of tDCS on basal activity levels—Virtual sensors were extracted from peak brain responses in the occipital cortices (i.e., near the anode). Briefly, for each frequency bin, a one-sample t-test was conducted across all participants and the peak voxel was extracted from each hemisphere (i.e., left and right occipital cortices). At the alpha ERD peaks, the active group had significantly greater absolute alpha activity (i.e., not baseline-corrected) bilaterally compared to the sham group across the whole time series (all *p's* < .02, corrected; see Figure 5), which suggests a major shift in basal alpha activity. Conversely, induced alpha activity (i.e., relative to baseline) did not differ between groups. In other words, active stimulation resulted in a global increase in alpha activity in the occipital cortices, but this did not affect task-induced modulations (Figure 5). Interestingly, we also noted trending correlations between basal alpha activity and level of induced 30 Hz entrainment in the left occipital cortex, $r(32) = -.299$, $p = .066$, and right occipital cortex, $r(32) = -.313$, $p = .081$. No other group comparisons (basal or induced) in any other frequency bins were significant.

4. Discussion

In this study, we investigated the impact of tDCS on oscillatory activity in the occipital cortices (near the anode) and distant brain regions during a visual entrainment task that elicits simultaneous, robust neural responses in multiple discrete frequency bands (Heinrichs-Graham & Wilson, 2012). Participants received either active or sham tDCS using an occipital-frontal electrode configuration, and then underwent MEG during an offline visual entrainment task. We found that, after both active and sham stimulation, participants showed significant and widespread oscillatory entrainment at the fundamental flicker frequency (15 Hz), as well as multiple higher harmonics, similar to our previous work (Heinrichs-Graham & Wilson, 2012). Overall, the active group showed weaker synchronization (i.e., ERS) at the second harmonic (30 Hz) in occipital cortices, as well as altered oscillatory responses at 30 Hz in other brain regions (e.g., parietal), and in different brain regions at other frequencies. For example, the active tDCS group had significant desynchronization near the cathode at the fundamental, third harmonic, and fifth harmonic, which was absent in the sham group resulting in a significant group effect in the right IFG. The visual entrainment task also elicited robust ERD responses in the side-bands below (alpha) and above (beta) the fundamental frequency, which were generated primarily by the lateral occipital, parietal, and cerebellar cortices. Finally, virtual sensor analysis of peak activity in the occipital cortices showed a global increase in basal alpha activity in the active stimulation group compared to sham, which was not reflected in the stimulus-induced oscillatory responses (i.e., relative to baseline). Below we discuss the implications of this work for understanding the effects of tDCS on neurophysiology.

Before discussing our tDCS findings, we think it is important to consider the overall neurophysiological responses induced by this visual entrainment task. Our MEG analyses indicated that all participants (active and sham) had robust alpha and beta desynchronization (ERD), with significant synchronization (ERS) at the fundamental and higher harmonics of the visual flicker frequency, shortly after the onset of the visual stimulus in the occipital cortices. Greater ERD power was found in the lateral occipital cortices, while ERS entrainment responses peaked in the medial occipital cortices near the calcarine fissure. Given the highly synchronous spontaneous alpha rhythm that occurs in the occipital cortices at rest (Betti et al., 2013; Brookes et al., 2011), it is possible that a subpopulation of neurons in this region desynchronized at the alpha frequency and simultaneously became entrained at the fundamental frequency or higher harmonics during visual processing. Interestingly, the peak alpha/beta desynchronization responses occurred lateral to the peaks of the entrainment frequencies, which would be expected since the visual stimulation was presented centrally (foveal). Presumably, neurons in lateral occipital cortices were desynchronized from their spontaneous alpha rhythm at the onset of visual stimulation, but were not directly driven by the visual stimulus due to their receptive field, and thus did not entrain at the flicker frequency or its harmonics. Rather, these lateral neurons may have remained desynchronized at the alpha/beta frequency because they were receiving feed-forward visual data from neurons directly driven by the flicker stimulation. Alternatively, these more lateral occipital neurons may remain desynchronized simply because the visual system is being actively stimulated, yet this stimulation is outside of their receptive fields.

As far as tDCS-related effects, anodal stimulation of the occipital cortices resulted in a global (basal) increase in alpha activity within these cortices. However, this increase in alpha did not affect the alpha desynchronization power induced by the stimulus (relative to baseline). Recently, it has been suggested that the amplitude of tDCS effects may be modulated by what the participant is doing during the stimulation (Fertonani & Miniussi, 2016). Participants were watching an animated movie during tDCS in the current study, and movie-watching has been shown to modulate alpha activity in the occipital cortices (Betti et al., 2013). Thus, the frequency specificity of this basal alpha finding may reflect that occipital alpha oscillations were directly modulated during stimulation, which resulted in a significant and broad change in the basal power at this frequency following the stimulation. This pattern compliments earlier findings from Marshall and colleagues (2015), who demonstrated that cathodal stimulation of the occipital cortices decreased basal alpha power, but did not impact induced activity. Interestingly, there was no significant difference in occipital alpha power between sham and anodal stimulation in their study, nor was there any region that showed differences in induced activity as a function of tDCS stimulation (i.e., anodal vs. cathodal vs. sham; (Marshall et al., 2015). However, their study employed 15 consecutive, pseudo-randomized blocks of either anodal, cathodal, or sham tDCS at 2 mA for only 2 minutes at a time, before shifting to a different stimulation condition (e.g., anodal tDCS stimulation for 2 minutes, followed by cathodal stimulation for 2 minutes, etc.). As such, it is possible that the duration and/or amplitude of stimulation in this study may have been insufficient to elicit neurophysiological effects in the oscillatory domain (Fertonani & Miniussi, 2016). Further, this study utilized a concurrent tDCSMEG protocol, whereas prior work has shown that the effect of tDCS may peak about 15-20 minutes after stimulation has stopped (Kuo et al., 2013; Nitsche et al., 2007), although these studies focused on excitability in the motor cortices and it is unclear how this temporal profile compares across anatomical targets.

The current findings also included significant reductions in ERS activity in occipital and parietal cortices in the active group compared to sham. Basically, the sham group showed a much more widespread synchronization throughout occipital and parietal regions at both the second and third harmonic, whereas activity in these frequency bands was much more limited in the active group. This contributed to the significantly reduced entrainment in the occipital cortices at the second harmonic (30 Hz) in the active compared to the sham group, which is particularly intriguing because visual entrainment at the second harmonic has been shown to be modulated by attention (Kim, Grabowecky, Paller, & Suzuki, 2011). Unfortunately, the functional role of the second and higher-order harmonics remains elusive, and most paradigms involving harmonic responses to date uses them as a stimulus-tagging method (Andersen, Fuchs, & Muller, 2011; Andersen, Muller, & Hillyard, 2015; J. Ding, Sperling, & Srinivasan, 2006; Itthipuripat, Garcia, & Serences, 2013; Muller et al., 2006; Ordikhani-Seyedlar, Sorensen, Kjaer, Siebner, & Puthusserypady, 2014; Scherbaum, Frisch, & Dshemuchadse, 2016; Toffanin, de Jong, Johnson, & Martens, 2009), with little discussion of their specific role in brain function. Nonetheless, taken together it is possible that the basal increase in absolute alpha amplitude, while not directly affecting the induced alpha oscillatory response amplitude, might have impeded the simultaneous entrainment of neurons to fundamental and harmonic frequencies. In other words, with stronger baseline

alpha synchrony, it is less likely that neurons would become entrained at other frequencies during stimulus presentation. This is somewhat supported by our finding of a relationship between basal alpha activity and induced 30 Hz ERS entrainment, though these correlations were only trending. Regardless, this hypothesis, while preliminary, could explain some of the variability in the tDCS results reported in neuroimaging research (see (Fertonani & Miniussi, 2016; Filmer et al., 2014; Horvath, Forte, & Carter, 2015)). At the very least, our data suggests that tDCS differentially modulates basal activity levels (e.g., during the baseline) and induced responses, and highlights the deceptively complicated nature of tDCS in the context of neurophysiology.

Finally, we also found multi-band desynchronizations in the right IFG in the active group that were absent in the sham group. This is an especially interesting finding and was likely due to cathodal stimulation of this region, as the cathode was placed directly above the right IFG. Importantly, electrode placement at this supraorbital region is often utilized as the "reference" in tDCS studies that focus on anodal effects (Fridriksson, Richardson, Baker, & Rorden, 2011; Grundmann et al., 2011; Hanley et al., 2015; Pavlova, Kuo, Nitsche, & Borg, 2014; Pellicciari, Brignani, & Miniussi, 2013; Penolazzi, Pastore, & Mondini, 2013; Raimundo, Uribe, & Brasil-Neto, 2012; Zheng, Alsop, & Schlaug, 2011), many others). These inferior frontal areas have been shown to be crucial to attention, especially in the context of visual attention and cognitive control (Cieslik, Mueller, Eickhoff, Langner, & Eickhoff, 2015). Thus, we hypothesize that numerous tasks that require attention, decision-making, or a quick reaction to a stimulus may be affected by such an electrode configuration, due to an unwanted change in the neurophysiology of the frontal cortices. More broadly, these results illuminate the importance of carefully considering the electrode configuration, and may hold implications for understanding some of the divergent findings in the tDCS literature on frontal lobe tasks (Tremblay et al., 2014). Future work should focus on understanding how the specific tDCS electrode montage may impact brain areas underlying and between both the anode and the cathode, especially when both electrodes are placed on the scalp (versus an extracephalic area such as the arm).

In conclusion, this study is the first to show that occipital tDCS significantly modulates neural oscillatory activity during an offline visual entrainment task. We found that anodal stimulation increased basal alpha power within the occipital cortices, but that this increase did not significantly affect oscillatory alpha responses. In addition, we found a significant reduction in neural entrainment at harmonics of the flicker frequency in the active compared to sham group, as well as significant ERD responses in the right inferior frontal cortices, proximal to the cathode, in the active group that were absent in the sham group. Taken together, it is possible that anodal tDCS of the occipital cortices results in an increase in spontaneous alpha activity, which may interfere with the entrainment of neuronal populations in response to the flicker frequency. These results also highlight the importance of carefully considering the impact of different electrode configurations on whole-brain dynamics. Limitations of the current study include no quantification of measures of attention during visual stimulation, and a lack of baseline (pre-stimulation) activity in both groups. Both of these measures would help clarify the mechanistic and functional role of active tDCS on visual oscillatory activity, and future studies should address these issues. Future work should also directly investigate the relationship between changes in spontaneous

oscillatory activity and induced oscillatory activity following tDCS, as well as the impact of electrode configuration, tDCS amplitude, and duration of stimulation on oscillatory rhythms.

Acknowledgements

This work was supported by NIH grant R01 MH103220 (TWW), NSF grant #1539067 (TWW), the Shoemaker Prize from the University of Nebraska Foundation (TWW), a Kinman-Oldfield Award for Neurodegenerative Research from the University of Nebraska Foundation (TWW), and a grant from the Nebraska Banker's Association (TWW).

References

Alekseichuk I, Diers K, Paulus W, Antal A. Transcranial electrical stimulation of the occipital cortex during visual perception modifies the magnitude of BOLD activity: A combined tES-fMRI approach. Neuroimage. 2015 doi: 10.1016/j.neuroimage.2015.11.034.

Amadi U, Ilie A, Johansen-Berg H, Stagg CJ. Polarity-specific effects of motor transcranial direct current stimulation on fMRI resting state networks. Neuroimage. 2013; 88C:155–161. doi: 10.1016/j.neuroimage.2013.11.037.

Andersen SK, Fuchs S, Muller MM. Effects of feature-selective and spatial attention at different stages of visual processing. J Cogn Neurosci. 2011; 23(1):238–246. doi: 10.1162/jocn.2009.21328. [PubMed: 19702461]

Andersen SK, Muller MM, Hillyard SA. Attentional Selection of Feature Conjunctions Is Accomplished by Parallel and Independent Selection of Single Features. J Neurosci. 2015; 35(27): 9912–9919. doi: 10.1523/jneurosci.5268-14.2015. [PubMed: 26156992]

Antal A, Kincses TZ, Nitsche MA, Bartfai O, Paulus W. Excitability changes induced in the human primary visual cortex by transcranial direct current stimulation: direct electrophysiological evidence. Invest Ophthalmol Vis Sci. 2004; 45(2):702–707. [PubMed: 14744917]

Antal A, Kincses TZ, Nitsche MA, Paulus W. Modulation of moving phosphene thresholds by transcranial direct current stimulation of V1 in human. Neuropsychologia. 2003; 41(13):1802–1807. [PubMed: 14527543]

Antal A, Nitsche MA, Kincses TZ, Kruse W, Hoffmann KP, Paulus W. Facilitation of visuo-motor learning by transcranial direct current stimulation of the motor and extrastriate visual areas in humans. Eur J Neurosci. 2004; 19(10):2888–2892. doi: 10.1111/j.1460-9568.2004.03367.x. [PubMed: 15147322]

Antal A, Polania R, Schmidt-Samoa C, Dechent P, Paulus W. Transcranial direct current stimulation over the primary motor cortex during fMRI. Neuroimage. 2011; 55(2):590–596. doi: 10.1016/j.neuroimage.2010.11.085. [PubMed: 21211569]

Barbieri M, Negrini M, Nitsche MA, Rivolta D. Anodal-tDCS over the human right occipital cortex enhances the perception and memory of both faces and objects. Neuropsychologia. 2016; 81:238–244. doi: 10.1016/j.neuropsychologia.2015.12.030. [PubMed: 26744225]

Betti V, Della Penna S, de Pasquale F, Mantini D, Marzetti L, Romani GL, Corbetta M. Natural scenes viewing alters the dynamics of functional connectivity in the human brain. Neuron. 2013; 79(4): 782–797. doi: 10.1016/j.neuron.2013.06.022. [PubMed: 23891400]

Brookes MJ, Woolrich M, Luckhoo H, Price D, Hale JR, Stephenson MC, Morris PG. Investigating the electrophysiological basis of resting state networks using magnetoencephalography. Proc Natl Acad Sci U S A. 2011; 108(40):16783–16788. doi: 10.1073/pnas.1112685108. [PubMed: 21930901]

Cieslik EC, Mueller VI, Eickhoff CR, Langner R, Eickhoff SB. Three key regions for supervisory attentional control: evidence from neuroimaging meta-analyses. Neurosci Biobehav Rev. 2015; 48:22–34. doi: 10.1016/j.neubiorev.2014.11.003. [PubMed: 25446951]

Coffman BA, Clark VP, Parasuraman R. Battery powered thought: enhancement of attention, learning, and memory in healthy adults using transcranial direct current stimulation. Neuroimage. 2014; 85(Pt 3):895–908. doi: 10.1016/j.neuroimage.2013.07.083. [PubMed: 23933040]

Ding J, Sperling G, Srinivasan R. Attentional modulation of SSVEP power depends on the network tagged by the flicker frequency. Cereb Cortex. 2006; 16(7):1016–1029. doi: 10.1093/cercor/bhj044. [PubMed: 16221931]

Ding Z, Li J, Spiegel DP, Chen Z, Chan L, Luo G, Thompson B. The effect of transcranial direct current stimulation on contrast sensitivity and visual evoked potential amplitude in adults with amblyopia. Sci Rep. 2016; 6:19280. doi: 10.1038/srep19280. [PubMed: 26763954]

Ernst MD. Permutation methods: A basis for exact inference. Stat Sci. 2004; 19:676–685.

Fertonani A, Miniussi C. Transcranial Electrical Stimulation: What We Know and Do Not Know About Mechanisms. Neuroscientist. 2016 doi: 10.1177/1073858416631966.

Filmer HL, Dux PE, Mattingley JB. Applications of transcranial direct current stimulation for understanding brain function. Trends Neurosci. 2014; 37(12):742–753. doi: 10.1016/j.tins.2014.08.003. [PubMed: 25189102]

Fridriksson J, Richardson JD, Baker JM, Rorden C. Transcranial direct current stimulation improves naming reaction time in fluent aphasia: a double-blind, sham-controlled study. Stroke. 2011; 42(3):819–821. doi: 10.1161/STROKEAHA.110.600288. [PubMed: 21233468]

Gall C, Silvennoinen K, Granata G, de Rossi F, Vecchio F, Brosel D, Sabel BA. Noninvasive electric current stimulation for restoration of vision after unilateral occipital stroke. Contemp Clin Trials. 2015; 43:231–236. doi: 10.1016/j.cct.2015.06.005. [PubMed: 26072125]

Garcia-Cossio E, Witkowski M, Robinson SE, Cohen LG, Birbaumer N, Soekadar SR. Simultaneous transcranial direct current stimulation (tDCS) and whole-head magnetoencephalography (MEG): assessing the impact of tDCS on slow cortical magnetic fields. Neuroimage. 2015 doi: 10.1016/j.neuroimage.2015.09.068.

Gross J, Kujala J, Hamalainen M, Timmermann L, Schnitzler A, Salmelin R. Dynamic imaging of coherent sources: Studying neural interactions in the human brain. Proc Natl Acad Sci U S A. 2001; 98(2):694–699. doi: 10.1073/pnas.98.2.694. [PubMed: 11209067]

Grundmann L, Rolke R, Nitsche MA, Pavlakovic G, Happe S, Treede RD, Bachmann CG. Effects of transcranial direct current stimulation of the primary sensory cortex on somatosensory perception. Brain Stimul. 2011; 4(4):253–260. doi: 10.1016/j.brs.2010.12.002. [PubMed: 22032740]

Hanley CJ, Singh KD, McGonigle DJ. Transcranial modulation of brain oscillatory responses: A concurrent tDCS-MEG investigation. Neuroimage. 2015 doi: 10.1016/j.neuroimage.2015.12.021.

Heinrichs-Graham E, Wilson TW. Presence of strong harmonics during visual entrainment: a magnetoencephalography study. Biol Psychol. 2012; 91(1):59–64. doi: 10.1016/j.biopsycho.2012.04.008. [PubMed: 22569101]

Hilgenstock R, Weiss T, Huonker R, Witte OW. Behavioural and neurofunctional impact of transcranial direct current stimulation on somatosensory learning. Hum Brain Mapp. 2016; 37(4):1277–1295. doi: 10.1002/hbm.23101. [PubMed: 26757368]

Hillebrand A, Singh KD, Holliday IE, Furlong PL, Barnes GR. A new approach to neuroimaging with magnetoencephalography. Hum Brain Mapp. 2005; 25(2):199–211. doi: 10.1002/hbm.20102. [PubMed: 15846771]

Horvath JC, Forte JD, Carter O. Evidence that transcranial direct current stimulation (tDCS) generates little-to-no reliable neurophysiologic effect beyond MEP amplitude modulation in healthy human subjects: A systematic review. Neuropsychologia. 2015; 66:213–236. doi: 10.1016/j.neuropsychologia.2014.11.021. [PubMed: 25448853]

Hunter MA, Coffman BA, Gasparovic C, Calhoun VD, Trumbo MC, Clark VP. Baseline effects of transcranial direct current stimulation on glutamatergic neurotransmission and large-scale network connectivity. Brain Res. 2015; 1594:92–107. doi: 10.1016/j.brainres.2014.09.066. [PubMed: 25312829]

Itthipuripat S, Garcia JO, Serences JT. Temporal dynamics of divided spatial attention. J Neurophysiol. 2013; 109(9):2364–2373. doi: 10.1152/jn.01051.2012. [PubMed: 23390315]

Jasper HH. The ten-twenty electrode system of the International Federation. Electroencephalography and Clinical Neurophysiology. 1958; 10:371–375.

Kim YJ, Grabowecky M, Paller KA, Suzuki S. Differential roles of frequency-following and frequency-doubling visual responses revealed by evoked neural harmonics. J Cogn Neurosci. 2011; 23(8):1875–1886. doi: 10.1162/jocn.2010.21536. [PubMed: 20684661]

Klem GH, Luders HO, Jasper HH, Elger C. The ten-twenty electrode system of the International Federation. The International Federation of Clinical Neurophysiology. Electroencephalogr Clin Neurophysiol Suppl. 1999; 52:3–6. [PubMed: 10590970]

Kraft A, Roehmel J, Olma MC, Schmidt S, Irlbacher K, Brandt SA. Transcranial direct current stimulation affects visual perception measured by threshold perimetry. Exp Brain Res. 2010; 207(3-4):283–290. doi: 10.1007/s00221-010-2453-6. [PubMed: 21046369]

Kuo HI, Bikson M, Datta A, Minhas P, Paulus W, Kuo MF, Nitsche MA. Comparing cortical plasticity induced by conventional and high-definition 4 × 1 ring tDCS: a neurophysiological study. Brain Stimul. 2013; 6(4):644–648. doi: 10.1016/j.brs.2012.09.010. [PubMed: 23149292]

Lang N, Siebner HR, Chadaide Z, Boros K, Nitsche MA, Rothwell JC, Antal A. Bidirectional modulation of primary visual cortex excitability: a combined tDCS and rTMS study. Invest Ophthalmol Vis Sci. 2007; 48(12):5782–5787. doi: 10.1167/iovs.07-0706. [PubMed: 18055832]

Liebetanz D, Nitsche MA, Tergau F, Paulus W. Pharmacological approach to the mechanisms of transcranial DC-stimulation-induced after-effects of human motor cortex excitability. Brain. 2002; 125(Pt 10):2238–2247. [PubMed: 12244081]

Makovski T, Lavidor M. Stimulating occipital cortex enhances visual working memory consolidation. Behav Brain Res. 2014; 275:84–87. doi: 10.1016/j.bbr.2014.09.004. [PubMed: 25205369]

Maris E, Oostenveld R. Nonparametric statistical testing of EEG- and MEG-data. J Neurosci Methods. 2007; 164(1):177–190. doi: 10.1016/j.jneumeth.2007.03.024. [PubMed: 17517438]

Marshall TR, Esterer S, Herring JD, Bergmann TO, Jensen O. On the relationship between cortical excitability and visual oscillatory responses - A concurrent tDCS-MEG study. Neuroimage. 2015 doi: 10.1016/j.neuroimage.2015.09.069.

Muller MM, Andersen S, Trujillo NJ, Valdes-Sosa P, Malinowski P, Hillyard SA. Feature-selective attention enhances color signals in early visual areas of the human brain. Proc Natl Acad Sci U S A. 2006; 103(38):14250–14254. doi: 10.1073/pnas.0606668103. [PubMed: 16956975]

Nitsche MA, Doemkes S, Karakose T, Antal A, Liebetanz D, Lang N, Paulus W. Shaping the effects of transcranial direct current stimulation of the human motor cortex. J Neurophysiol. 2007; 97(4): 3109–3117. doi: 10.1152/jn.01312.2006. [PubMed: 17251360]

Nitsche MA, Liebetanz D, Lang N, Antal A, Tergau F, Paulus W. Safety criteria for transcranial direct current stimulation (tDCS) in humans. Clin Neurophysiol. 2003; 114(11):2220–2222. author reply 2222-2223. [PubMed: 14580622]

Nitsche MA, Nitsche MS, Klein CC, Tergau F, Rothwell JC, Paulus W. Level of action of cathodal DC polarisation induced inhibition of the human motor cortex. Clin Neurophysiol. 2003; 114(4):600–604. [PubMed: 12686268]

Nitsche MA, Paulus W. Excitability changes induced in the human motor cortex by weak transcranial direct current stimulation. J Physiol. 2000; 527(Pt 3):633–639. [PubMed: 10990547]

Nitsche MA, Paulus W. Sustained excitability elevations induced by transcranial DC motor cortex stimulation in humans. Neurology. 2001; 57(10):1899–1901. [PubMed: 11723286]

Okamoto M, Dan H, Sakamoto K, Takeo K, Shimizu K, Kohno S, Dan I. Three-dimensional probabilistic anatomical cranio-cerebral correlation via the international 10-20 system oriented for transcranial functional brain mapping. Neuroimage. 2004; 21(1):99–111. [PubMed: 14741647]

Okamoto M, Dan I. Automated cortical projection of head-surface locations for transcranial functional brain mapping. Neuroimage. 2005; 26(1):18–28. doi: 10.1016/j.neuroimage.2005.01.018. [PubMed: 15862201]

Olma MC, Kraft A, Roehmel J, Irlbacher K, Brandt SA. Excitability changes in the visual cortex quantified with signal detection analysis. Restor Neurol Neurosci. 2011; 29(6):453–461. doi: 10.3233/RNN-2011-0607. [PubMed: 22278016]

Ordikhani-Seyedlar M, Sorensen HB, Kjaer TW, Siebner HR, Puthusserypady S. SSVEP-modulation by covert and overt attention: Novel features for BCI in attention neurorehabilitation. Conf Proc IEEE Eng Med Biol Soc. 2014; 2014:5462–5465. doi: 10.1109/embc.2014.6944862. [PubMed: 25571230]

Papp N, Ktonas P. Critical evaluation of complex demodulation techniques for the quantification of bioelectrical activity. Biomed Sci Instrum. 1977; 13:135–145. [PubMed: 871500]

Pavlova E, Kuo MF, Nitsche MA, Borg J. Transcranial direct current stimulation of the premotor cortex: effects on hand dexterity. Brain Res. 2014; 1576:52–62. doi: 10.1016/j.brainres.2014.06.023. [PubMed: 24978602]

Pellicciari MC, Brignani D, Miniussi C. Excitability modulation of the motor system induced by transcranial direct current stimulation: a multimodal approach. Neuroimage. 2013; 83:569–580. doi: 10.1016/j.neuroimage.2013.06.076. [PubMed: 23845429]

Penolazzi B, Pastore M, Mondini S. Electrode montage dependent effects of transcranial direct current stimulation on semantic fluency. Behav Brain Res. 2013; 248:129–135. doi: 10.1016/j.bbr.2013.04.007. [PubMed: 23597838]

Plow EB, Obretenova SN, Fregni F, Pascual-Leone A, Merabet LB. Comparison of visual field training for hemianopia with active versus sham transcranial direct cortical stimulation. Neurorehabil Neural Repair. 2012; 26(6):616–626. doi: 10.1177/1545968311431963. [PubMed: 22291042]

Plow EB, Obretenova SN, Jackson ML, Merabet LB. Temporal profile of functional visual rehabilitative outcomes modulated by transcranial direct current stimulation. Neuromodulation. 2012; 15(4):367–373. doi: 10.1111/j.1525-1403.2012.00440.x. [PubMed: 22376226]

Poline JB, Worsley KJ, Holmes AP, Frackowiak RS, Friston KJ. Estimating smoothness in statistical parametric maps: variability of p values. J Comput Assist Tomogr. 1995; 19(5):788–796. [PubMed: 7560327]

Poreisz C, Boros K, Antal A, Paulus W. Safety aspects of transcranial direct current stimulation concerning healthy subjects and patients. Brain Res Bull. 2007; 72(4-6):208–214. doi: 10.1016/j.brainresbull.2007.01.004. [PubMed: 17452283]

Raimundo RJ, Uribe CE, Brasil-Neto JP. Lack of clinically detectable acute changes on autonomic or thermoregulatory functions in healthy subjects after transcranial direct current stimulation (tDCS). Brain Stimul. 2012; 5(3):196–200. doi: 10.1016/j.brs.2011.03.009. [PubMed: 22037121]

Reinhart RM, Woodman GF. Enhancing long-term memory with stimulation tunes visual attention in one trial. Proc Natl Acad Sci U S A. 2015; 112(2):625–630. doi: 10.1073/pnas.1417259112. [PubMed: 25548192]

Reinhart RM, Zhu J, Park S, Woodman GF. Synchronizing theta oscillations with direct-current stimulation strengthens adaptive control in the human brain. Proc Natl Acad Sci U S A. 2015; 112(30):9448–9453. doi: 10.1073/pnas.1504196112. [PubMed: 26124116]

Renzi C, Ferrari C, Schiavi S, Pisoni A, Papagno C, Vecchi T, Cattaneo Z. The role of the occipital face area in holistic processing involved in face detection and discrimination: A tDCS study. Neuropsychology. 2015; 29(3):409–416. doi: 10.1037/neu0000127. [PubMed: 25110932]

Scherbaum S, Frisch S, Dshemuchadse M. Switches of stimulus tagging frequencies interact with the conflict-driven control of selective attention, but not with inhibitory control. Int J Psychophysiol. 2016; 99:103–107. doi: 10.1016/j.ijpsycho.2015.11.012. [PubMed: 26592667]

Soekadar SR, Witkowski M, Cossio EG, Birbaumer N, Robinson SE, Cohen LG. In vivo assessment of human brain oscillations during application of transcranial electric currents. Nat Commun. 2013; 4:2032. doi: 10.1038/ncomms3032. [PubMed: 23787780]

Spiegel DP, Byblow WD, Hess RF, Thompson B. Anodal transcranial direct current stimulation transiently improves contrast sensitivity and normalizes visual cortex activation in individuals with amblyopia. Neurorehabil Neural Repair. 2013; 27(8):760–769. doi: 10.1177/1545968313491006. [PubMed: 23774122]

Stagg CJ, Nitsche MA. Physiological basis of transcranial direct current stimulation. Neuroscientist. 2011; 17(1):37–53. doi: 10.1177/1073858410386614. [PubMed: 21343407]

Strigaro G, Mayer I, Chen JC, Cantello R, Rothwell JC. Transcranial Direct Current Stimulation Effects on Single and Paired Flash Visual Evoked Potentials. Clin EEG Neurosci. 2015; 46(3):208–213. doi: 10.1177/1550059414539481. [PubMed: 25253432]

Taulu S, Simola J. Spatiotemporal signal space separation method for rejecting nearby interference in MEG measurements. Phys Med Biol. 2006; 51(7):1759–1768. doi: 10.1088/0031-9155/51/7/008. [PubMed: 16552102]

Taulu S, Simola J, Kajola M. Applications of the signal space separation method (SSS). IEEE Trans Signal Process. 2005; 53(9):3359–3372.

Toffanin P, de Jong R, Johnson A, Martens S. Using frequency tagging to quantify attentional deployment in a visual divided attention task. Int J Psychophysiol. 2009; 72(3):289–298. [PubMed: 19452603]

Tremblay S, Lepage JF, Latulipe-Loiselle A, Fregni F, Pascual-Leone A, Theoret H. The uncertain outcome of prefrontal tDCS. Brain Stimul. 2014; 7(6):773–783. doi: 10.1016/j.brs.2014.10.003. [PubMed: 25456566]

Uusitalo MA, Ilmoniemi RJ. Signal-space projection method for separating MEG or EEG into components. Med Biol Eng Comput. 1997; 35(2):135–140. [PubMed: 9136207]

Van Veen BD, van Drongelen W, Yuchtman M, Suzuki A. Localization of brain electrical activity via linearly constrained minimum variance spatial filtering. IEEE Trans Biomed Eng. 1997; 44(9): 867–880. doi: 10.1109/10.623056. [PubMed: 9282479]

Wilson TW, Kurz MJ, Arpin DJ. Functional specialization within the supplementary motor area: a fNIRS study of bimanual coordination. Neuroimage. 2014; 85(Pt 1):445–450. doi: 10.1016/j.neuroimage.2013.04.112. [PubMed: 23664948]

Woods AJ, Antal A, Bikson M, Boggio PS, Brunoni AR, Celnik P, Nitsche MA. A technical guide to tDCS, and related non-invasive brain stimulation tools. Clin Neurophysiol. 2016; 127(2):1031–1048. doi: 10.1016/j.clinph.2015.11.012. [PubMed: 26652115]

Worsley KJ, Andermann M, Koulis T, MacDonald D, Evans AC. Detecting changes in nonisotropic images. Hum Brain Mapp. 1999; 8(2-3):98–101. [PubMed: 10524599]

Worsley KJ, Marrett S, Neelin P, Vandal AC, Friston KJ, Evans AC. A unified statistical approach for determining significant signals in images of cerebral activation. Hum Brain Mapp. 1996; 4(1):58–73. doi: 10.1002/(SICI)1097-0193(1996)4:1<58::AID-HBM4>3.0.CO;2-O 10.1002/(SICI)1097-0193(1996)4:1<58::AID-HBM4>3.0.CO;2-O. [PubMed: 20408186]

Zheng X, Alsop DC, Schlaug G. Effects of transcranial direct current stimulation (tDCS) on human regional cerebral blood flow. Neuroimage. 2011; 58(1):26–33. doi: 10.1016/j.neuroimage.2011.06.018. [PubMed: 21703350]

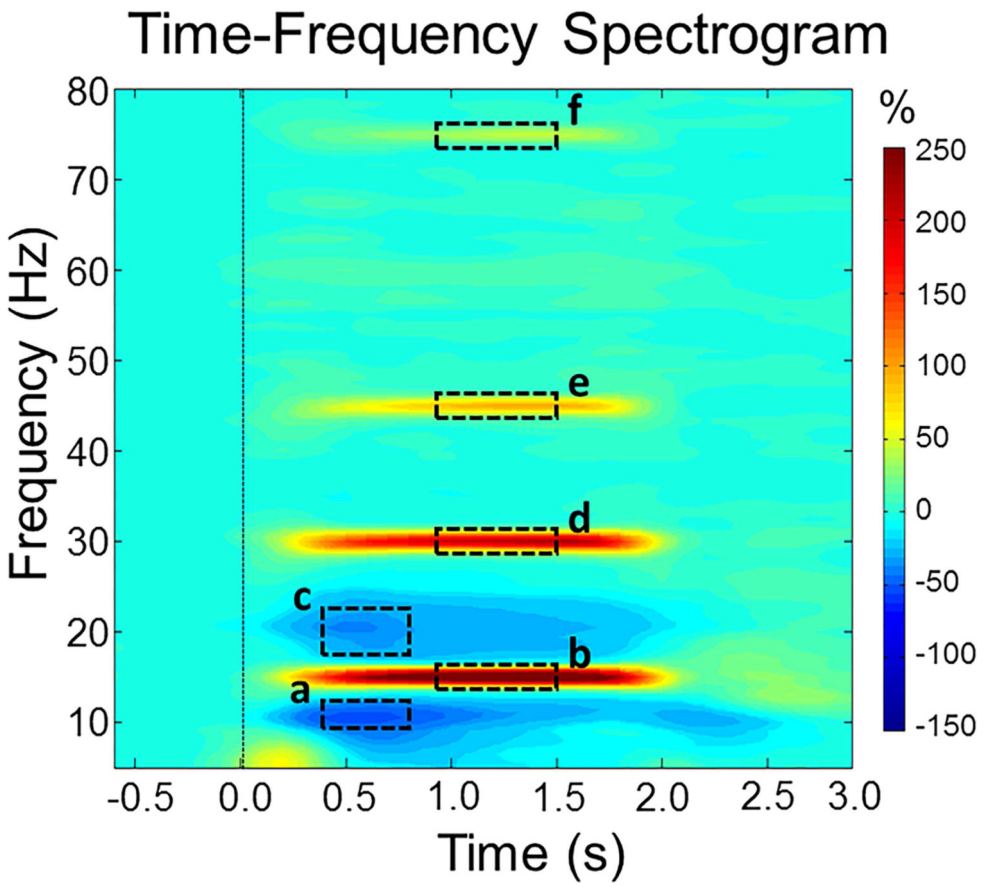

Figure 1. Group-averaged time-frequency spectra during visual entrainment

Time (s) is denoted on the x-axis, with 0.0 s defined as stimulus onset. Frequency (Hz) is shown on the y-axis. All signal power data is expressed as a percent difference from baseline, with the color legend shown to the far right. The baseline was defined as −0.6 to 0.0 s before stimulus onset. Data represent a group-averaged gradiometer near the medial occipital cortex averaged across all participants (the same sensor was selected in each participant) in the active and sham groups. As can be discerned, the visual flicker stimulus resulted in entrainment at the fundamental frequency (15 Hz), as well as the second harmonic (30 Hz), third harmonic (45 Hz), and fifth harmonic (75 Hz). Significant entrainment was unable to be resolved at 60 Hz, likely because this is the mains power frequency in the United States. There were also significant desynchronization responses found in the alpha and beta frequencies. Dotted boxes denote the time-frequency bins that were imaged using beamforming for the a) alpha ERD, b) fundamental, c) beta ERD, d) second harmonic, e) third harmonic, and f) fifth harmonic.

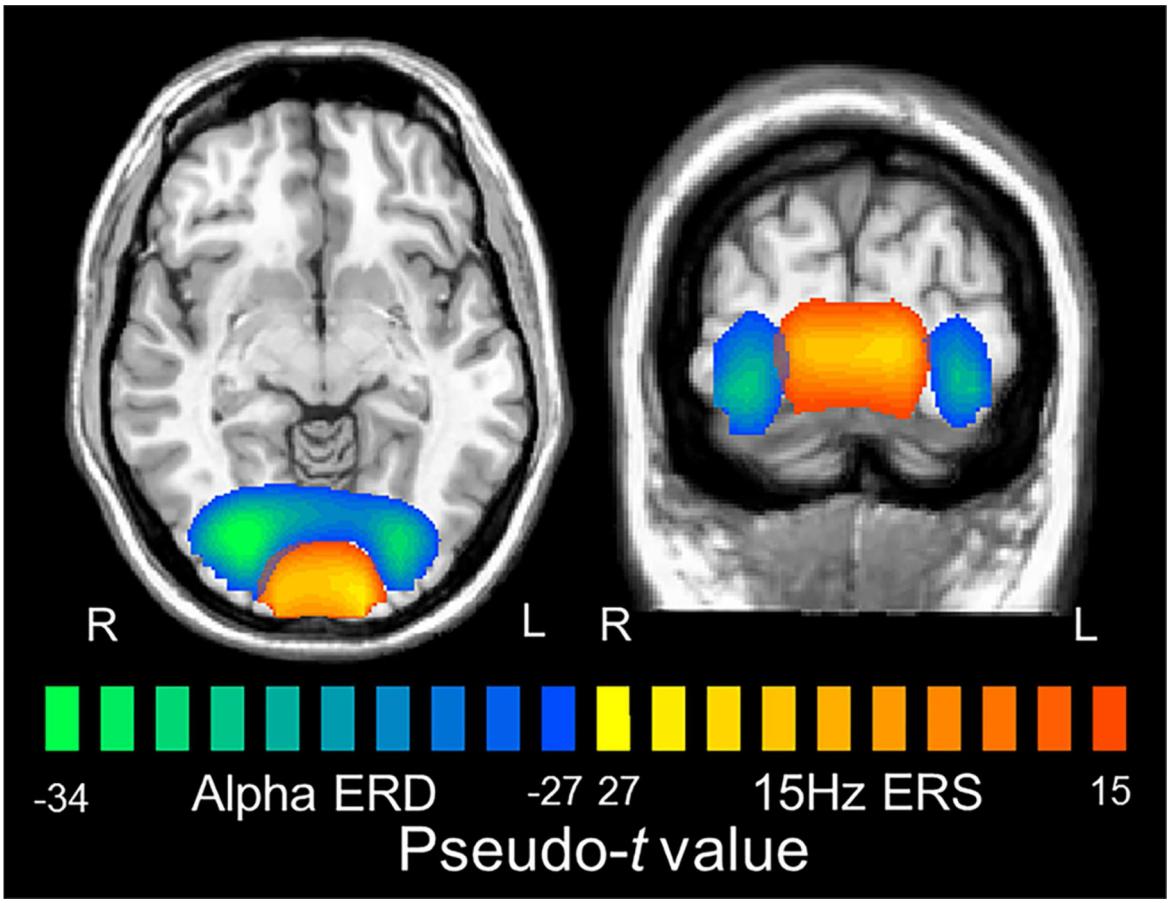

Figure 2. Spatial relationship of occipital responses at alpha and fundamental frequencies

Mean beamformer images (pseudo-*t*; see color bars) of the alpha ERD (0.4 to 0.8 s, 10-13 Hz) and fundamental ERS (0.9 to 1.5 s, 14-16 Hz) collapsed across the two groups. As can be discerned, fundamental ERS responses peaked in the medial occipital cortices, while the alpha ERD responses peaked more laterally. Of note, the peaks for the beta ERD were similar to those of the alpha ERD, while the harmonic ERS responses (not shown) were spatially-concordant with the fundamental ERS response.

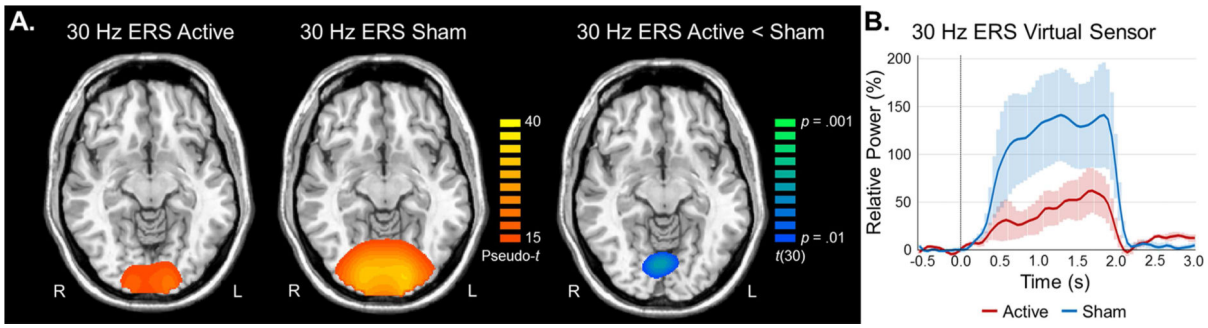

Figure 3. Effects of tDCS on the second harmonic ERS response

A) Group mean beamformer images (pseudo-*t*; see left color bar) of the 30 Hz ERS response are shown for the active (left image) and sham (middle image) groups individually, while the statistical map (active vs. sham) is shown on the right (corrected *p*-values; see right color bar). The active group had significantly reduced ERS responses compared to the sham group in the medial occipital cortices ($p < .01$, corrected; right image). Axial slices are shown in radiologic convention (right = left). **B)** Virtual sensor time series data is shown for the peak voxel of the statistical map, with the sham group data appearing in blue and the active group shown with a red line. Shaded areas denote SEM.

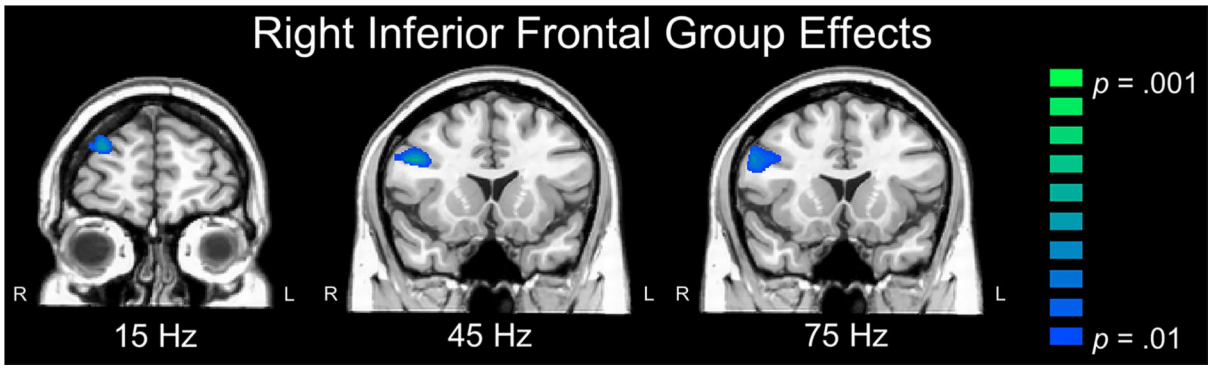

Figure 4. Effects of cathodal stimulation on the right frontal cortices

Color bars to the right denote image thresholds (*p*-values) and all images reflect areas of stronger ERD in the active compared to the sham group. Coronal slices are shown in radiologic convention (right = left). Participants in the active group had a significant ERD in the right inferior frontal gyrus at the fundamental (15 Hz), third harmonic (45 Hz) and fifth harmonic (75 Hz), which resulted in significant group effects in this region at these frequencies ($p < .01$, corrected).

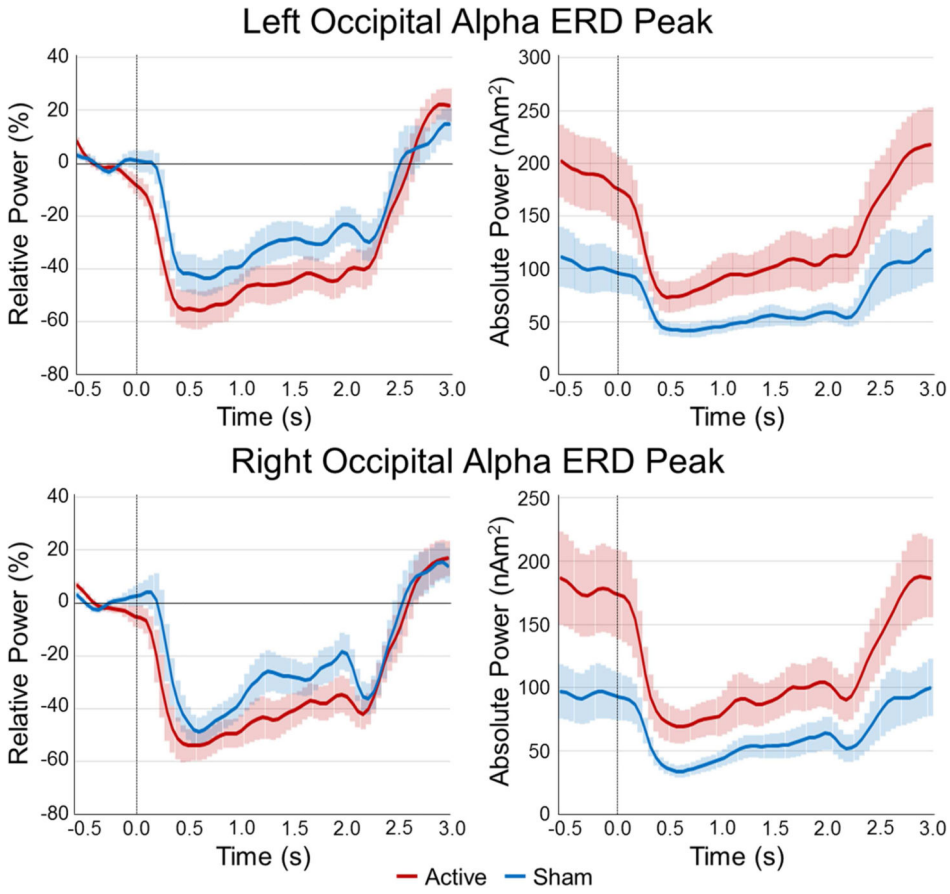

Figure 5. Absolute and relative temporal evolution of the alpha visual response

Voxel time series were extracted from the peak voxels of the left occipital cortex (top panel) and right occipital cortex (bottom panel) to more precisely examine the dynamics of the alpha ERD in the active (red line) and sham groups (blue line). Time (in s, stimulus onset = 0.0 s) is denoted on the x-axis, while power is shown on the y-axis. The left panel shows each response as a percentage relative to baseline (−0.6 to 0.0 s), while the right panel shows the absolute power (in nAm^2). Participants in the active group had significantly stronger basal alpha power ($p < .001$, corrected), but this did not impact task-induced oscillatory alpha responses (relative to baseline). The shaded area around each line denotes the SEM.

Table 1

Significant ERS and ERD Responses.

Response	Task Effects: Active	ERD/ERS	Task Effects: Sham	ERD/ERS	Group Difference	Direction
14-16 Hz,	R occipital	ERS	R occipital	ERS	n.s.	
0.9 – 1.5 s	L occipital	ERS	L occipital	ERS	n.s.	
	R inferior frontal gyrus	ERD	--	--	$p < .01$	Active ERD, Sham n.s.
29-31 Hz,	R occipital	ERS	R occipital	ERS	$p < .01$	ERS: Sham > Active
0.9 – 1.5 s	L occipital	ERS	L occipital	ERS	$p < .01$	ERS: Sham > Active
	R cerebellum	ERS	R cerebellum	ERS	n.s.	
	L cerebellum	ERS	L cerebellum	ERS	n.s.	
	L superior frontal gyrus	ERS	L superior frontal gyrus	ERS	n.s.	
	--	--	L dorsolateral PFC	ERS	n.s.	
	--	--	L SMA	ERS	$p < .01$	Sham ERS, Active n.s.
	--	--	R SMA	ERS	n.s.	
	--	--	Medial PFC	ERS	$p < .01$	Sham ERS, Active n.s.
	--	--	R precentral gyrus	ERS	n.s.	
	--	--	R posterior parietal	ERS	$p < .01$	Sham ERS, Active n.s.
	--	--	R middle occipital gyrus	ERS	n.s.	
44-46 Hz,	R occipital	ERS	R occipital	ERS	n.s.	
0.9 – 1.5 s	L occipital	ERS	L occipital	ERS	n.s.	
	R cerebellum	ERS	R cerebellum	ERS	n.s.	
	L cerebellum	ERS	L cerebellum	ERS	n.s.	
	Posterior cingulate	ERS	Posterior cingulate	ERS	n.s.	
	R posterior parietal	ERS	R posterior parietal	ERS	$p < .01$	ERS: Sham > Active
	R inferior frontal gyrus	ERD	--	--	$p < .01$	Active ERD, Sham n.s.
74-76 Hz,	R occipital	ERS	R occipital	ERS	n.s.	
0.9 – 1.5 s	L occipital	ERS	L occipital	ERS	n.s.	
	R cerebellum	ERS	R cerebellum	ERS	n.s.	
	L cerebellum	ERS	L cerebellum	ERS	n.s.	
	R inferior frontal gyrus	ERD	--	--	$p < .01$	Active ERD, Sham n.s.
	--	--	R precentral gyrus	ERS	$p < .01$	Sham ERS, Active n.s.
	R dorsolateral PFC	ERD	--	--	n.s.	
10-13 Hz,	R occipital	ERD	R occipital	ERD	n.s.	
0.4 – 0.8 s	L occipital	ERD	L occipital	ERD	n.s.	
	R cerebellum	ERD	R cerebellum	ERD	n.s.	
	L cerebellum	ERD	L cerebellum	ERD	n.s.	
	R parietal	ERD	R parietal	ERD	n.s.	
	L parietal	ERD	L parietal	ERD	n.s.	
17-22 Hz,	R occipital	ERD	R occipital	ERD	n.s.	
0.4 – 0.8 s	L occipital	ERD	L occipital	ERD	n.s.	

Response	Task Effects: Active	ERD/ERS	Task Effects: Sham	ERD/ERS	Group Difference	Direction
	R cerebellum	ERD	R cerebellum	ERD	n.s.	
	L cerebellum	ERD	L cerebellum	ERD	n.s.	
	R parietal	ERD	R parietal	ERD	n.s.	
	L parietal	ERD	L parietal	ERD	n.s.	
	Medial PFC	ERD	--	--	$p < .01$	Active ERD, Sham n.s.
	--	--	L inferior temporal gyrus	ERD	$p < .01$	Sham ERD, Active n.s.
	--	--	R inferior temporal gyrus	ERD	n.s.	